Molecular Engineering of Ruthenium Sensitizers in Dye-Sensitized Solar Cells

Puhui Xie and Fengqi Guo[*]

Department of Chemistry, Zhengzhou University, Zhengzhou, Henan 450052, P.R.China

Abstract: Dye sensitized solar cells (DSSCs) have great potential to challenge the traditional silicon-based semiconductor solar cells in the photovoltaic (PV) market because of their low cost and medium efficiency. This type of solar cell has achieved an impressive photo-to-energy conversion efficiency of over 10%. In a dye sensitized solar cell, the charge separation is initiated at the adsorbed dye, which was bound at the interface of an inorganic semiconductor film and a hole transport material. The dye is the key component in such cells. In order to optimize the performance of such devices, it is important to design suitable dyes with tunable spectroscopic and electrochemical properties. Careful modification of the structures of the sensitizers can improve light harvesting in the visible and near-IR region with high optical extinction co-efficients and enhance the performance of the devices. It's necessary to optimize the properties of the dye in conjunction with other factors in order to best exploit and be fully compatible with other cell modifications in the development of cheap and efficient photovoltaic systems. In this review, current strategies for the molecular engineering of the dyes based on ruthenium complexes possessing different functionalized ligands are discussed.

1. INTRODUCTION

The energy sources are very important for the worldwide technological and economic development. The traditional energy sources based on fossil fuels (such as oil, gas, coal) have to be replaced by some new energy systems in the future in view of the limited reserves, the global warming and the air pollution. Sustainable and renewable energy will certainly serve as the major clean energy sources to be widely used for the future. Solar photovoltaic cells, capable of directly converting solar energy into electricity, provide a direct approach for the usage of renewable energy. As a new generation of photovoltaics, dye sensitized solar cells (DSSCs) have great potential to challenge the traditional silicon-based semiconductor solar cells in the photovoltaic (PV) market because of their low cost and medium efficiency [1-7].

1.1. Operation of Dye Sensitized Solar Cells (DSSCs)

The operation of a DSSC is based on the new concepts of nanotechnology and molecular engineering. The device comprises two primary parts: a photoanode and a counterelectrode sandwiching an electrolyte medium (usually a solution containing I_3^-/I^- couple). The photoanode is made of SnO_2:F deposited on the back of a transparent conducting plate(FTO), on the back of which is sintered with a thin layer of TiO_2. A thin layer of the dye is attached to the outside surface of the TiO_2 film. And the photoinert counter electrode is another conducting plate with a thin layer of catalyst (usually platinum). The two parts are then joined and sealed together to prevent the electrolyte from leaking.
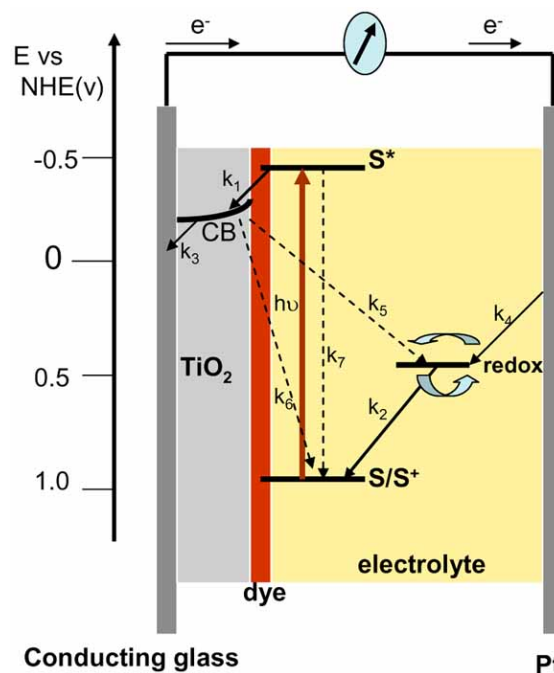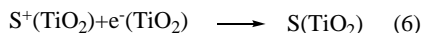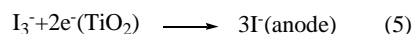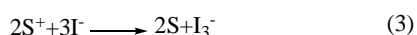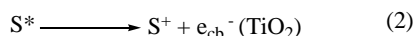

Fig. (1). Operation of a DSSC (S=sensitizer; potentials are referred to the normal hydrogen electrode (NHE)). The green arrows represent processes required for photovoltaic function: k_1=charge injection, k_2=dye regeneration, k_3=charge collection at the conducting glass electrode, and k_4=charge collection at the Pt electrode. The black arrows represent loss mechanisms: k_5=charge recombination with a hole transport material (dark current), k_6=charge recombination with the oxidized sensitizer (S^+), and k_7=decay of the excited state of the sensitizer (S^*).

The operating principles of the DSSC are presented schematically in Fig. (**1**) and the processes for the photocurrent generation are listed from eq.1 to eq.4 [8]. Photoexcitation of the sensitizer promotes an electron to its excited state (eq. **1**), from which the electron is injected into the conduc-

*Address correspondence to this author at the Department of Chemistry, Zhengzhou University, Zhengzhou, Henan 450052, China. Tel: 086-0371-67783126; Fax: 086-0371-67781250; E-mail: fqguo@zzu.edu.cn

tion band of the oxide (eq. **2**). The ground state of the dye is regenerated by the electron donation from the electrolyte (eq. **3**) or a solid-state or quasi-solid-state (gel) material. The iodide is regenerated by the reduction of triiodide at the counter electrode (usually a Pt electrode) (eq. **4**) and the circuit is completed *via* electron migration through the external load. However, there are undesirable side reactions: the injected electrons may recombine either with triiodide at the TiO$_2$ surface (eq. **5**), or with oxidized sensitizer (eq. **6**), resulting in losses in the cell efficiency. Therefore the processes of eqs. (**2**) and (**3**) must be kinetically more favorable than those of eqs. (**5**) and (**6**) in order to get stable photocurrent.

$$S + h\upsilon \longrightarrow S^* \qquad (1)$$

$$S^* \longrightarrow S^+ + e_{cb}^-(TiO_2) \qquad (2)$$

$$2S^+ + 3I^- \longrightarrow 2S + I_3^- \qquad (3)$$

$$I_3^- + 2e \longrightarrow 3I^- \qquad (4)$$

$$I_3^- + 2e^-(TiO_2) \longrightarrow 3I^-(anode) \qquad (5)$$

$$S^+(TiO_2) + e^-(TiO_2) \longrightarrow S(TiO_2) \qquad (6)$$

1.2. Key Parameters for the Performance of a DSSC

The performance of a solar cell is defined by the following key parameters, **i**) the short circuit current (I_{sc}); **ii**) the open circuit voltage (V_{oc}) generated under standard illumination conditions (AM 1.5, intensity of incident light $I_s = 1000W\ cm^{-2}$); **iii**) the fill factor (FF) of the cell under AM 1.5 illumination. These parameters can be obtained by a full current-voltage characterization, which is the essential measure of the diode behavior of a cell. The FF can be calculated *via*

$$FF = P_{max}/V_{oc}I_{sc} = (VI)_{max}/V_{oc}I_{sc} \qquad (7)$$

iv) The incident photon conversion efficiency (IPCE), which shows the wavelength dependence of a DSSC. The value at a given illumination wavelength λ with an incident optical power P_{in} is derived from the following equation

$$IPCE = e\lambda P_{in}/hcI_{sc} \qquad (8)$$

Where e is the fundamental electronic charge, h is Planck's constant and c is the speed of light in vacuum; **v**) the overall power conversion efficiency (η) of a cell producing electrical power under standard AM1.5 illumination conditions. η is given by:

$$\eta = I_{sc}V_{oc}FF/P_{in} \qquad (9)$$

2. MOLECULAR ENGINEERING OF RUTHENIUM COMPLEXES AS PHOTOSENSITIZERS FOR DSSCS

In order to achieve high performance of the DSSCs, it's necessary to prepare the sensitizers with tunable spectroscopic and electrochemical properties by systematically modifying the structure of the sensitizers. Further efforts have to be made to develop novel sensitizers with an increased optical cross section, and the light-harvesting spectra of the sensitizers can spread over a wide range to encompass

as much of the visible and near-IR spectrum as possible. Thus, the dyes used in DSSCs technology must accomplish a number of essential engineering requirements. 1) They must have an anchoring group to bind strongly to TiO$_2$ film. 2) The LUMO of the dye must be sufficiently high in energy for efficient charge injection into the TiO$_2$ conduction band (when compared to the lifetime of any other relaxation or quenching processes), and the HOMO must be sufficiently low in energy for efficient regeneration of the ground state of the dye by the redox couple [9]. 3) The dye must have strong absorption and cover a broad range in solar spectrum. 4) The sensitizer must be capable of many reduction and oxidation cycles without decomposition. Many cheap organic photosensitizers including porphyrins [10, 11], phthalocyanines [12], viologens [13, 14], rhodamine [15], xanthene dyes [16], organic aromatic hydrocarbons [17, 18], coumarin [19], squaraine [20], indoline [21], hemicyanine [22] and some natural sensitizers [23-27] have been investigated for semiconductor sensitizations. The highest efficiency reported was about 8% [21]. However, the aggregation and the poor stabilities of the dyes would limit their practical application in solar cells.

2.1. The Star Sensitizer of N3 for DSSCs

Among the photosensitizers explored, the most useful sensitizers for thin film electrodes are metal complexes of polypyridines because of their strong absorption in the visible region and long excited states lifetimes. In addition, they are stable in oxidized and reduced forms, and do not have the tendency to aggregate or decompose [28]. Their photophysical and electrochemical properties can be finely tuned by varying the metals and the ligands.
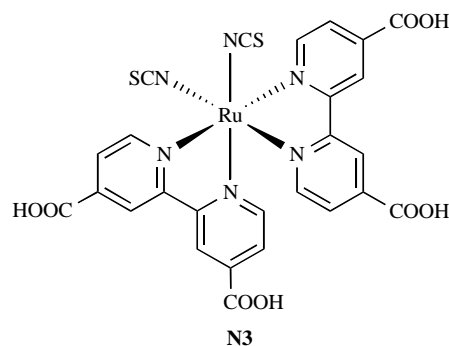

Fig. (2). The star sensitizer *cis*-[Ru(dcbH$_2$)$_2$(NCS)$_2$] (**N3**) employed in DSSCs.

A magnificent achievement in DSSCs has been made by the Grätzel group [1, 29-30]. Under the AM 1.5 illumination, the cell based on a mesoscopic titania film attached with *cis*-di(thiocyanato)bis(2,2'-bipyridyl-4,4'-dicarboxylic acid) ruthenium(II) *cis*-(Ru(dcbH$_2$)$_2$(NCS)$_2$ (Fig. **2**), coded as **N3,** generated a short circuit current density of 16 mA·cm^{-2}, an open circuit voltage of 0.7 V and a maximum overall power conversion efficiency of 10.4% by using iodine/iodide as redox mediator [31]. The photocurrent action spectrum of **N3** dominated almost the entire visible region with *IPCE* of 90% between 500 and 600nm. Many laboratories could reach efficiencies of 6-8% under similar conditions [32-35]. There-

fore, the **N3** complex is famous for the star sensitizer, which holds the record in power conversion efficiency for DSSCs. In such cells, the **N3** dye is anchored to the titania surface through the carboxylate groups in the 2,2'-bipyridyl ligands. The lowest excited state of **N3** is the metal-to-ligand charge-transfer (MLCT) state, in which an excited electron is transferred from the metal center to the π* system of the 2,2'-bipyridyl-4,4'-dicarboxylate ligand. The electron is subsequently injected into the titania conduction band within femto to picoseconds with near unity quantum yield of producing free charge (as shown in Fig. **3**). This is in part expected for the high reducing ability of the ³MLCT state (ca.-1 V versus SCE) of **N3** and its positive ground-state oxidation potential (+0.86V versus SCE). The role of the thiocyanato ligands in **N3** is to tune the t_{2g} orbital of ruthenium (II) and to stabilize the hole that is being generated on the metal after one electron was injected into the conduction band. This fact suggests that the key processes in function of the solar cell depend on the peculiar molecular property of the *cis*-[Ru(dcbH₂)₂(NCS)₂] complex.
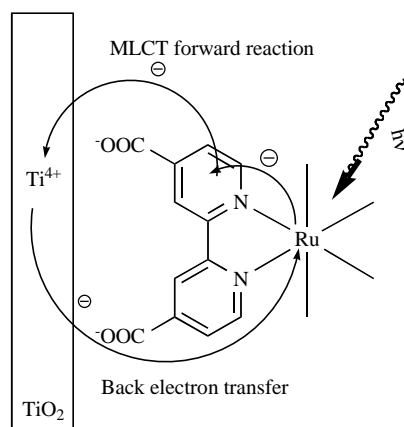

Fig. (3). Interfacial electron transfer process involving **N3** bound to the surface of the TiO₂ film.

However, there are some challenging issues on the **N3** dye based DSSCs. The first issue is the panchromatic sensitization of large band-gap mesoscopic semiconductor electrodes. Although the performance of the **N3** dye showed best so far, low IPCE values in the red and near-infrared region limited its application as a panchromatic sensitizer. The second issue is the development of sensitizers with high molar extinction coefficients. In **N3** based DSSCs, a film with thickness of 15 microns and a volatile redox electrolyte were required to achieve its performance. The third issue is the stability of the sealed cell. The long term containment at elevated temperatures of the volatile solvent mixture still remains a major challenge of the stability of the dye [36].

Carefully designed photosensitizers can be useful to tuning their spectroscopic properties, to preventing aggregation of the chromophores, and to establishing models for interfacial electron transfer studies. More generally, molecular engineering of Ru complexes seems to be a promising method for understanding the electron transfer processes at the molecule–nanoparticle interface, so that the electron transfer processes could be controlled in a rational and predictable

manner. Based on this idea, a series of ruthenium (II) complexes with 4,4'-dicarboxylic acid-2,2'-bipyridine(dcbH₂) and thiocyanato ligands (NCS) (i.e. the **N3** analogues) have been designed, and their spectroscopic properties and photovoltaic performances have been investigated. Several typical functional ligands were listed in Fig. (**4**).

## 2.2. Approaches to Bind the Sensitizers to the TiO₂ Film

Metal complex sensitizers for DSSCs usually have anchoring ligands and ancillary ligands (examples shown in Fig. **5**). Anchoring ligands of the complex are responsible for adsorption onto the semiconductor surface and are also chromophoric groups. Ancillary ligands are not directly attached onto the surface of the semiconductor. They are used for tuning the overall properties of the complexes. Ruthenium polypyridine complexes have been intensively employed as sensitizers due to their appropriate redox, spectroscopic, and excited-state properties [32-33, 37-42]. In particular ruthenium(II) complexes with carboxylic bipyridine ligands are able to react readily with oxide surfaces, presenting an efficient adsorption onto the semiconductor surface [43].

The anchoring ligands can immobilize the dye on nanocrystalline TiO₂ surface. It has been shown that the chemiadsorption at semiconductor oxide through carboxylic group can occur by a variety of binding modes (Fig. **6**), which depend on the structure of the dye, the binding groups, the pH value, and the preparation methods of the metal oxides [44].

The majority of dye molecules are bound to the surfaces of TiO₂ films through acidic groups—mostly carboxylic acid or phosphonic acid linkers [45]. Some other linkers like esters, acid chlorides, carboxylate salts, amides, sulphonic acid, silanes (SiX₃), ethers, acetylacetonate, salicylates and hydroxymethyl groups [46-48] were found to have poorer adsorption on semiconductor oxide surfaces compared to the carboxylic acid and phosphonic acid groups. The two ligands of 2,2'-bipyridyl-4,4'-dicarboxylic acid in the star molecule **N3** were the anchoring ligands in such DSSCs. The aim of incorporating carboxylic acid groups in the 4,4'-position of the 2,2'-bipyridine ligand is to graft the dye molecules on the semiconductor surface by forming ester linkages at the surface of the metal oxide and to provide intimate electronic coupling between the excited-state of the sensitizer and the conduction band of the semiconductor.

The sites of carboxylic groups on the 2,2'-bipyridyl ligand would affect the photophysical and photoelectric properties of the Ru(II) complexes [46, 49]. The Ru complexes with the carboxylic groups in the 3,3'-positions or 5,5'-positions of the 2,2'-bipyridyl ligand (Fig. **7**) exhibited poorer performance in both a dye-sensitized solar cell (Table **1**) [46] and a self-assembly monolayer (SAM) cell than the complex with the carboxylic groups in the 4,4'-positions [49]. The steric hindrance of the two carboxylic groups in the 3,3'-positions of *cis*-Ru(3,3'-dcbH₂)₂(NCS)₂ and the higher oxidation potential of the ground states of *cis*-Ru(5,5'-dcbH₂)₂(NCS)₂ were the reasons for the low DSSCs performance.
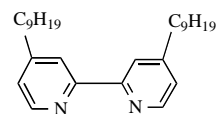
However, the platinum complex with carboxylic groups in the 3,3'-positions of 2,2'-bipyridyl showed the opposite effect with a slightly improved efficiency compared to the
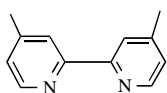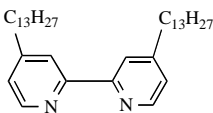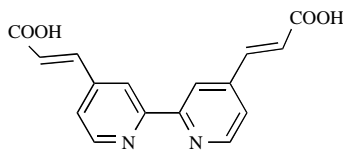
4,4'-dimethyl-2,2'-bipyridine(dmbpy)
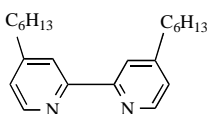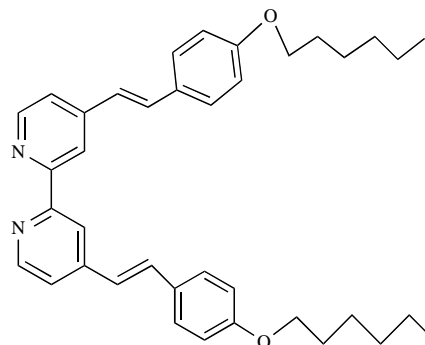
4,4'-dihexyl-2,2'-bipyridine(dhbpy)
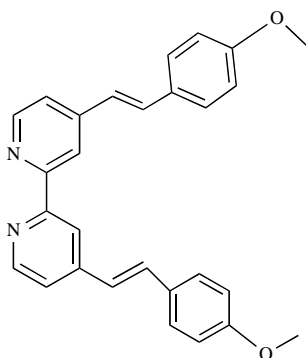
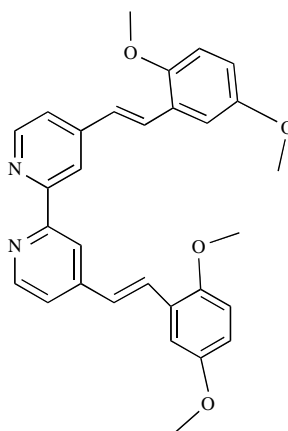4,4'-dinonyl-2,2'-bipyridine(dnbpy)

4,4'-ditridecyl-2,2'-bipyridine(dtdbpy)

4,4'-bis(carboxyvinyl)-2,2'-bipyridine

4,4'-bis(p-hexyloxystyryl)-2,2'-bipyridine

4,4'-bis(p-methoxystyryl)-2,2'-bipyridine

4,4'-di(2-(3,6-dimethoxyphenyl)-
ethenyl)-2,2'-bipyridine
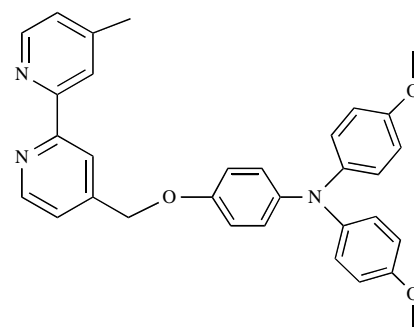
4-CH$_3$,4'-N,N-(di-p-anisylamino)phenoxy
methyl-2,2'-bipyridine
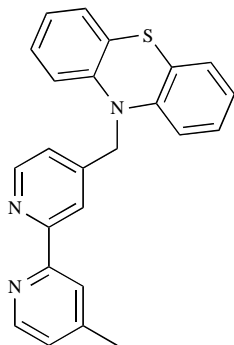
10-((2-(4-methylpyridin-2-yl)pyridin-4-yl)methyl)-
10*H*-phenothiazine

(4-CH$_3$,4'-CH$_2$-PTZ-2,2'-bipyridine)
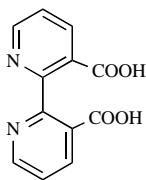
2,2'-bipyridyl-3,3'-dicarboxylic acid

(3,3'-dcbH$_2$)
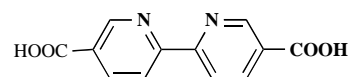
2,2'-bipyridyl-5,5'-dicarboxylic acid

(5,5'-dcbH$_2$)
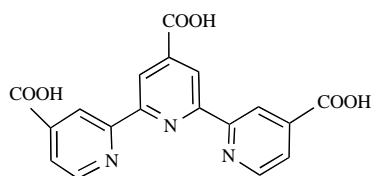
4,4',4"-tricarboxy-2,2':6',2"-terpyridine
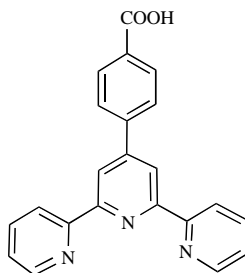
2,2':6',2"-terpyridine-4'-(4-carboxylic acid) phenyl

(ttp-COOH)
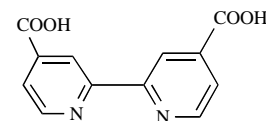
2,2'-bipyridyl-4,4'-dicarboxylic acid

(4,4'-dcbH$_2$)

Fig. (4). Contd…..

4,4'''-bis(t-butyl)-4',4''-bis(carboxymethyl)-
2,':6',2'':6'',2'''-quaterpyridine

diethyl 2,2':6',2'':6'',2'''-quaterpyridine-
4',4''-di-carboxylate

(detOq)

2,2'-bipyridyl-4,4'-diphosphonic acid

(bpy-(PO$_3$H$_2$)$_2$)

4'-phosphonic acid-2,2':6',2''-terpyridine

(hp-terpy)

2,2':6',2''-terpyridine-4'-(4-phosphonic acid) phenyl

(ttp-COOH)

2,2'-bipyridyl-4,4'-dihydroxy methyl

(bpy-CH$_2$OH)
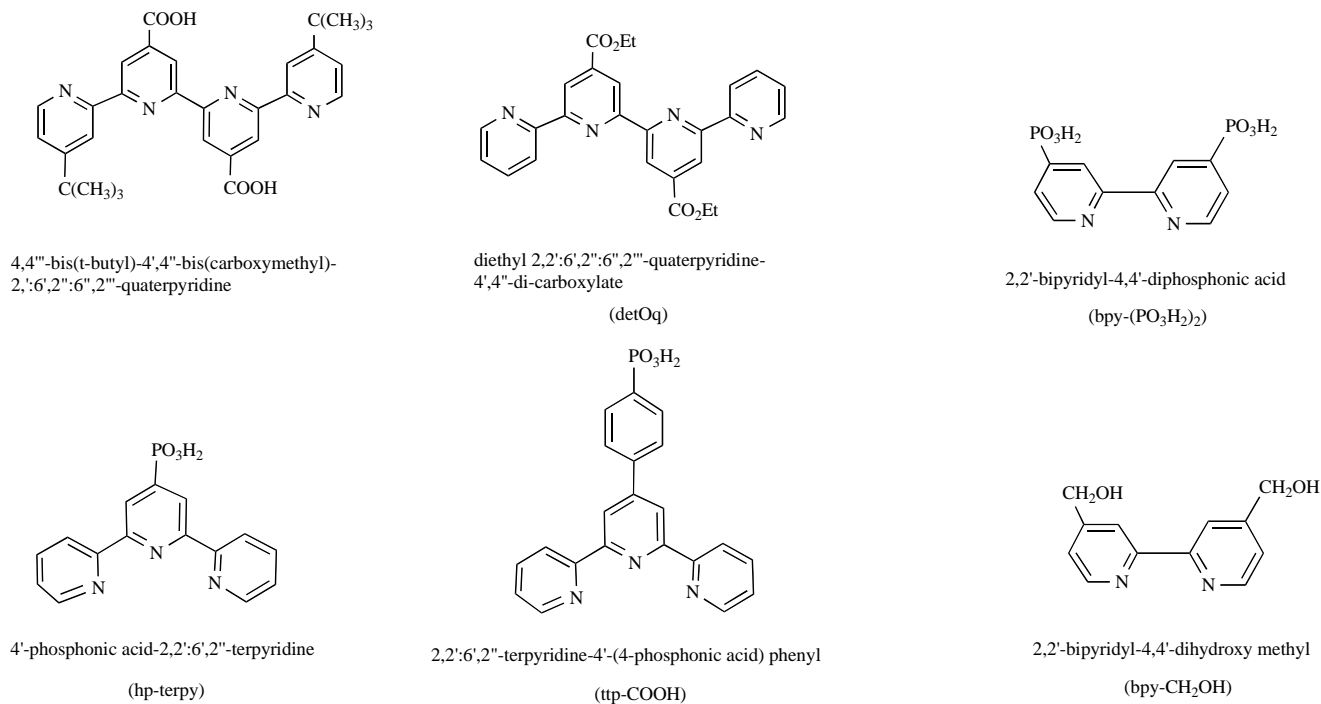
Fig. (4). Examples of functional ligands.

M=Ru(II), Os(II), Rh(III), Re(I), Cu(I)

L= [structure] Cl$^-$, CN$^-$, NCS$^-$, H$_2$O,Br$^-$,I$^-$, [structure]—R

A=COOH, P(O)(OH)$_2$
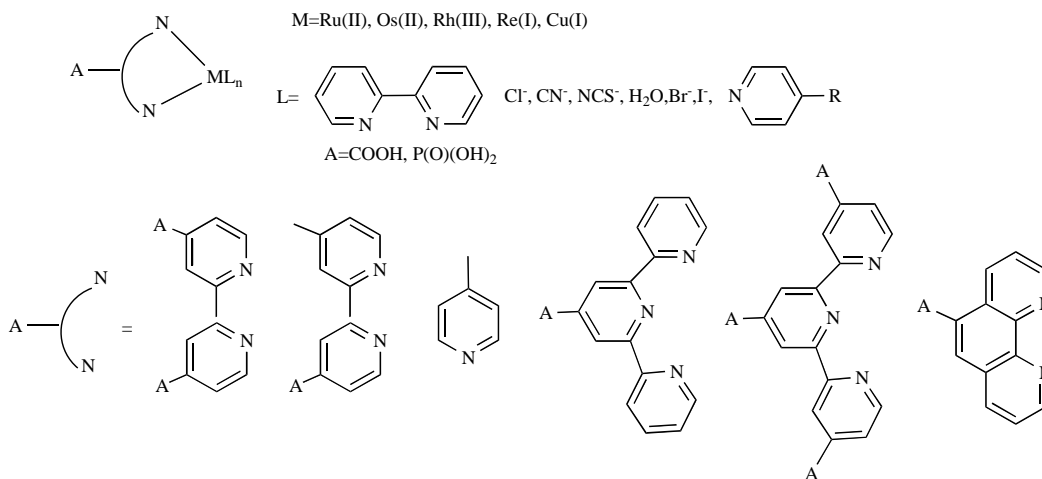
Fig. (5). Examples of metal complexes used for semiconductor sensitization in which the anchoring groups (**A**) are directly attached on the molecule's framework.

monodentate
ester-type

bidentate
chelating

bidentate
bridging

bidentate
bridging

H-bonded

H-bonded

carboxylate

monodentate
through CO
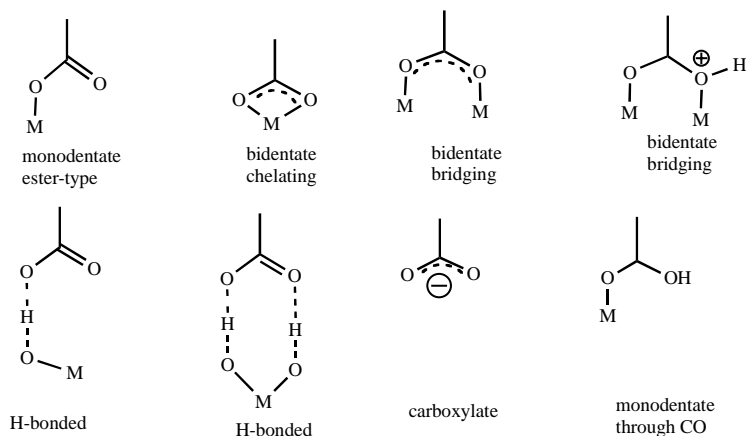
Fig. (6). Possible binding modes of a COOH group to a metal oxide (TiO$_2$).
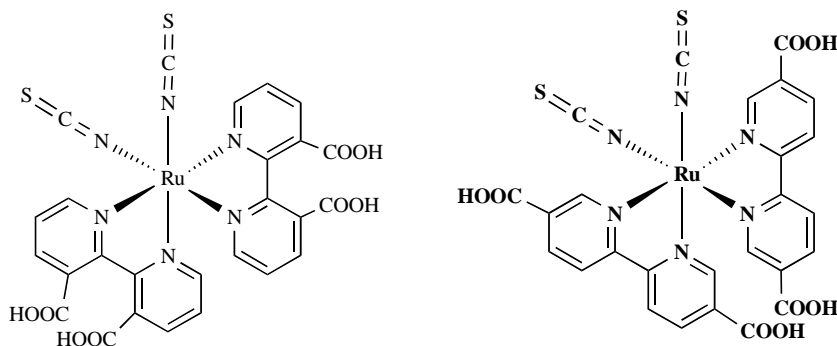
Fig. (7). cis-Ru(3,3'-dcbH$_2$)$_2$(NCS)$_2$ (Left) and cis-Ru(5,5'-dcbH$_2$)$_2$(NCS)$_2$.

Table 1. Photophysical, Electrochemical, and Photoelectrochemical Properties of the *cis*-Ru(LL)$_2$(NCS)$_2$ on TiO$_2$

Sensitizer	$\lambda_{abs.max}$ (nm)	E^o (V,vsSCE)	I_{sc} (mA/cm^2)	V_{oc} (V)	$10^7\Gamma$ (mol/cm^2)	LHE	max IPCE
Ru(3,3'-dcbH$_2$)$_2$(NCS)$_2$	570	0.87	8.0	0.47	1.69	0.824	0.213
Ru(4,4'-dcbH$_2$)$_2$(NCS)$_2$	535	0.85	18.4	0.57	2.10	0.951	0.671
Ru(5,5'-dcbH$_2$)$_2$(NCS)$_2$	580	0.95	7.8	0.49	2.10	0.806	0.366

other two complexes with the carboxylic groups in the 4,4'-positions or 5,5'-positions [50].

The first sensitizer bearing the phosphonic acid anchoring group was a ruthenium terpyridyl complex [51, 52]. The performance was obtained with IPCE values up to 70%. They appear to be promising candidates to compete with the carboxylated analogous [52]. Further modifications on the phosphonated-terpy ligand by introducing a phenyl group close to the anchoring group provided an even better complex for sensitizing TiO$_2$ with a maximum IPCE value of 75.6% [53].

Gillaizeau-Gauthier *et al.* [54] investigated the influence of the position of the phosphonic acid group (4,4'- versus 5,5'-), and the presence of methylene spacer between the bpy ligand and the phosphonic acid group (–CH$_2$PO$_3$H$_2$ versus –PO$_3$H$_2$) on the performance of some ruthenium complexes containing phosphonic acid substituted bipyridine. The photoelectrochemical performances on transparent TiO$_2$ films showed that the change in position from 4,4'-to 5,5'- decreased the IPCE values. This fact is in the same trend with the analogous complexes bearing carboxylic acid groups [46, 55]. The introduction of a methylene spacer also decreased the IPCE values most probably due to a reduced electronic coupling between excited state of the dye and the conduction band of the semiconductor. The best sensitizer within this series is *cis*-[Ru(4,4'-(PO$_3$H$_2$)$_2$-bpy)$_2$(NCS)$_2$] (Fig. **8**). However, this complex displayed a ca. 30% lower overall efficiency compared to the carboxylated analogue due to the blue shifted absorption spectrum, which caused a decrease of the light harvesting efficiency in the longer wavelength region [56].

The highest efficiency (at least 8%) for a Ru complex with a non-carboxylic acid linker was reported in a recent investigation into phosphonic acid anchoring groups (**Z955** [45]) (Fig. **9**). Modification of the linker from carboxylic to phosphonic acid groups resulted in an interrelated series of changes in the characteristics of the device. For example, the absorption maximum of the lowest MLCT band for **Z955** was blue-shifted. And the DSSCs based on **Z955** has a better stability and a slower charge-recombination kinetics than those of the analogous dye with carboxylic acid linkers (**Z907** (Fig. **9**), a heteroleptic analogue of **N3**. The increased number of protons on the phosphonic acid groups compared with carboxylic acid groups has been proposed as a factor in modifying the properties of the dye.

The absorption spectrum of the phosphonated complex is blue-shifted compared to the carboxylated species (Table **2**) because the phosphonic acid substituents can destabilize the LUMO energy level. This difference is due to the fact that the sp^3 hybridization of the phosphorous atom in –PO$_3$H$_2$ does not favor the interactions with the bpy core, while the structure of co-planarity between the sp^2 hybridized carbonyl carbon and the pyridine ring favors the interaction.

Changing the protonation of the acid groups had influence on the efficiency of the solar cell. The deprotonated **N3**,
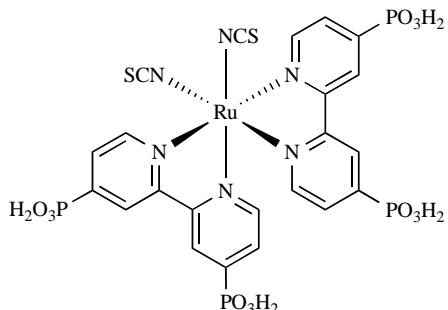

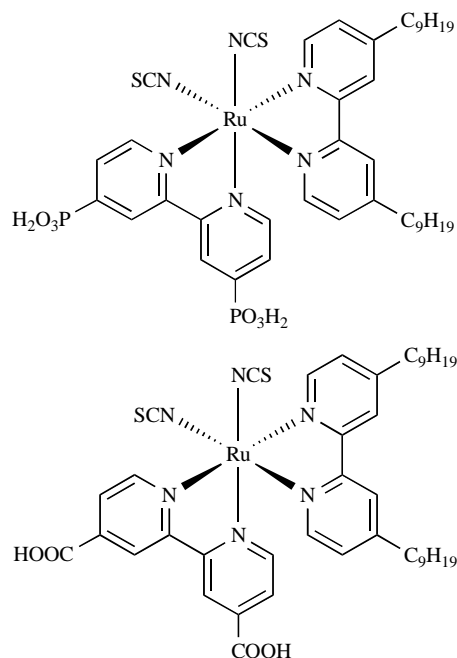**Fig. (8).** *cis*-Ru(4,4'- (PO$_3$H$_2$)$_2$-bpy)$_2$(NCS)$_2$.

Fig. (9). The typical amphiphilic dyes **Z955** (up) and **Z907** (down).

N719 (Fig. **10**) performed a higher cell efficiency than **N3** due to the effect of the bounded dye on the energy of the TiO$_2$ conduction band [57]. Thus, the nature of the anchoring group between the dye and the TiO$_2$ can play a crucial role in the optimization of the cell performance.
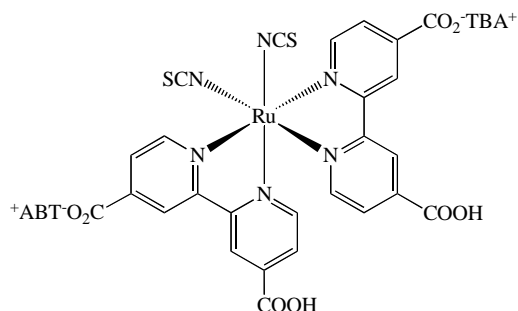

Fig. (10). The **N719**.

2.3. Panchromatic Sensitization for the DSSC

Although scientists have made great progress in the pioneering studies on dye sensitized nanocrystalline TiO$_2$ films using **N3** or **N719**, the main disadvantages of these sensitizers were the weak absorption in the red region of the solar spectrum and the relatively low molar extinction coefficient [31]. Many efforts have been made to overcome these shortcomings without significant success [55, 58-60]. Several stringent requirements of the DSSCs sensitizers, including absorbing all the visible light and functioning as an efficient charge-transfer sensitizer, present a challenging task for molecular engineering of ruthenium complexes on TiO$_2$-based DSSCs. In order to develop sensitizers with all the requirements satisfied simultaneously, it is necessary to investigate the relationship between the structures and photoelectric properties of the sensitizers. For example, the energy of the

LUMO and HOMO of the sensitizers (Fig. **11**) should be maintained at levels where photoinduced electron transfer into the TiO$_2$ conduction band and regeneration of the ground state dye by iodide can take place at practically 100% yield.
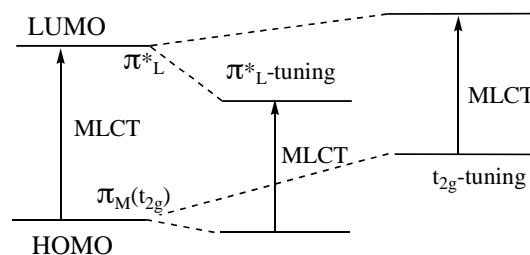

Fig. (11). Schematic representation of effect of tuning HOMO and LUMO energy level on the energy of metal to ligand charge transfer (MLCT).

2.3.1. Tuning the HOMO Energy Level (t_{2g}-Tuning)

The energies of the metal-to-ligand charge transfer (MLCT) states can be modified systematically by changing the ancillary ligands. The MLCT absorption bands of the bis-chelated complexes, *cis*-[Ru(dcbH$_2$)$_2$(L)$_2$] (L = Cl$^-$, Br$^-$, I$^-$, NCS$^-$ and CN$^-$), shift to lower energy by changing L from π accepting ligands to the π donating ones. This is the effect due to a direct perturbation of the electronic density at the metal center (increasing the HOMO level). With the decrease in ligand field strength, the $E_{1/2}$ value of Ru(III)/(II) decreases in the order of CN > NCS > halides [31].

No better ligands than NCS have been found for the sensitizers to improve the overall efficiency or IPCE values of the DSSCs based on the series of *cis*-[Ru(dcbH$_2$)$_2$LL'] (where LL' are the ancillary ligands) [61-64], even though they usually provide a wider coverage of light harvesting in the lower energy region.

One manner to control the t_{2g} level involves the development of the *trans*-isomer of **N3** (*trans*-di(thiocyanato)-bis(2,2'-bipyridyl-4,4'-dicarboxylate) ruthenium(II), abbreviated to be *trans*-Ru [65, 66]). The lowest MLCT absorption maximum shifts from 538 to 582 nm upon *cis*-to-*trans* isomerization (Fig. **12**). This red-shift is attributed to the destabilization of the ruthenium t_{2g} orbital or due to the electron donation from the two anionic NCS ligands of the *trans*-isomer to ruthenium center. The cell fabricated with TiO$_2$ film sensitized by this *trans*-Ru generated a short-circuit photocurrent of 19.6 mA cm^{-2}, an open-circuit photovoltage of 720 mV (Fig. **12**) and an overall power conversion efficiency of 8.6% in simulated AM 1.5 solar light (Table **2**), while the cell based on *cis*-Ru generated 14.9 mA cm^{-2} of I_{sc}, 692 mV of V_{oc} and 0.60 of *FF*, corresponding to an overall power conversion efficiency of η 6.7% under similar condition [65]. However, such disadvantages as poor solubility and the tendency to photoinduced isomerization for the *trans*-Ru complex would limit its practical application.

With the inspiration of the triplet emitters applied in organic light-emitting diodes (OLEDs), several groups began to develop heavy-metal-containing complexes as sensitizers for DSSCs, of which the triplet states were involved in the
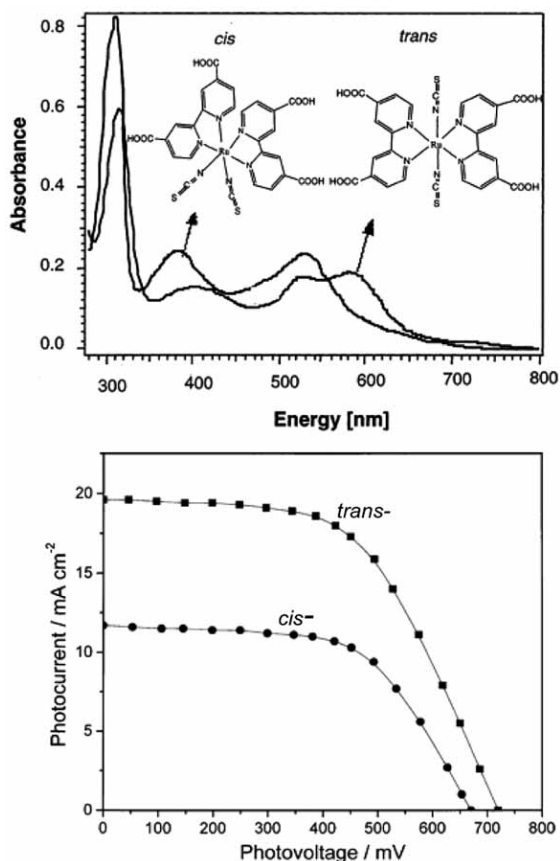
Fig. (12). Absorption spectra (left) and I-V curves comparisons of *cis*-Ru and *trans*-Ru(right).

photoinduced electron transfer (PET) process. The efficiency for generating long-lived charge separation is higher when the excited state that precedes PET is a spin triplet state. Thus the overall efficiency of the DSSCs should be improved in theory. A DSSC based on an osmium complex, $[Os(H_3tcterpy)(CN)_3]^-$, where $H_3tcterpy$ is 4,4',4''-tricarboxy-2,2':6',2''-terpyridine (Fig. **13**), with the lowest MLCT absorption band at 811 nm, presented better performance in the near-IR region than the corresponding Ru complex, although the Ru complex based cell performed better in the whole spectral region. The $[Os(H_3tcterpy)(CN)_3]^-$ complex can be chosen as a candidate for the development of osmium-based sensitizers where triplet state transitions could play a fundamental role in extending the spectral response in the near-IR region for photoelectrochemical applications [67].

Significant results have also been reported by Lewis's group on Os(II) complexes with dcbH$_2$ chromophoric ligand [68, 69]. Replacement of the ruthenium metal center with osmium extends the spectral response of nanocrystalline TiO$_2$ photoelectrodes to longer wavelengths without reducing the overall photo-electronic conversion efficiency. In these systems, direct population of low energy ^{3}MLCT states is less forbidden, allowing the presence of the corresponding charge transfer bands in the visible and near infrared region. These results predicted the possibility of further improving the performances of DSSCs by design of sensitizers with high spin–orbit coupling constants.
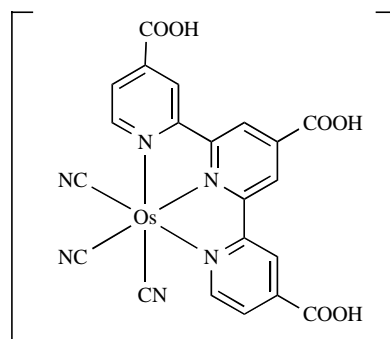

Fig. (13). Sensitizer with absorptions in the near-IR region compared to **N3**.

2.3.2. Tuning the LUMO Energy Level (π*-Tuning)

Tuning the LUMO energy levels of the sensitizers is another approach to develop dyes with intense absorption in the red region. The DSSC based on a "**black dye**" (Fig. **14**) presents an overall efficiency of 10.4% with a response extending into the near-IR region up to 920 nm [30].

A Ru tetrapyridyl dye with *trans* geometry for the two NCS ligands (Ru(detOq)(NCS)$_2$, where detOq= 4',4''-diethoxycarbonyl-2,2':6',2'':6'',2'''-quaterpyridine (Fig. **14**) [70] displayed a lower-energy absorption in comparison with **N3**, due to the decrease of the LUMO energy (Table **2**).

Wang *et al*. [34] designed a novel terpyridyl ruthenium complex $[Ru(ttp-COOH)(NCS)_3]^-$ (where ttp-COOH is 2,2':6',2''-terpyridine -4'-(4-carboxylic acid), Fig. **14**). The DSSC based on this dye generated *IPCE* values of about 90% at maximum photocurrent action spectra (580nm) and above 20% in the near-IR region. This red-shift is due to the more electronic delocalization of the terpyridyl ligand compared to the bipyridyl ligands. A sandwich-type solar cell fabricated with this dye-sensitized nanocrystalline TiO$_2$ film generated a short-circuit photocurrent of 6.1 mAcm^{-2}, an open-circuit photovoltage of 0.58 V and an overall yield of 2.9% under irradiation of white light (78.0 mW·cm^{-2}) (Table **2**). Since this dye responded better than the **N3** dye in the near-IR region, it would be a promising panchromatic sensitizer after optimization.

The absorption spectrum of the *trans*-[Ru(L)(NCS)$_2$], L = 4,4'''-di-tert-butyl-4',4''- bis(carboxylic acid)-2,2':6',2'':6'', 2'''-quaterpyridine (**N886**) (Fig. **14**) displays metal-to-ligand charge-transfer transitions in the entire visible region [71]. The panchromatic response of **N886** indicated a suitable sensitizer for DSSCs. The DSSCs based on **N886**, with an electrolyte containing 0.60 M butylmethylimidazolium iodide, 0.03 M I$_2$, and 0.50 M tert-butylpyridine in a mixture of acetonitrile and valeronitrile (volume ratio 1:1), generated a maximum incident photon-to-current efficiencies of 40%, a short-circuit photocurrent density of 11.8 mA/cm^2, an open-circuit voltage of 680 mV, and a fill factor of 0.73, corresponding to an overall conversion efficiency of 5.85% under AM 1.5 sunlight (Table **2**).

Recently, Klein et al have succeeded in fine-tuning the spectroscopic properties of ruthenium polypyridyl complexes by designing the novel ligand, 4,4'-bis(carboxyvinyl)-2, 2'-bipyridine and its ruthenium(II) complex [RuL$_2$(NCS)$_2$]

Black dye

Ru(detQq)(NCS)$_2$

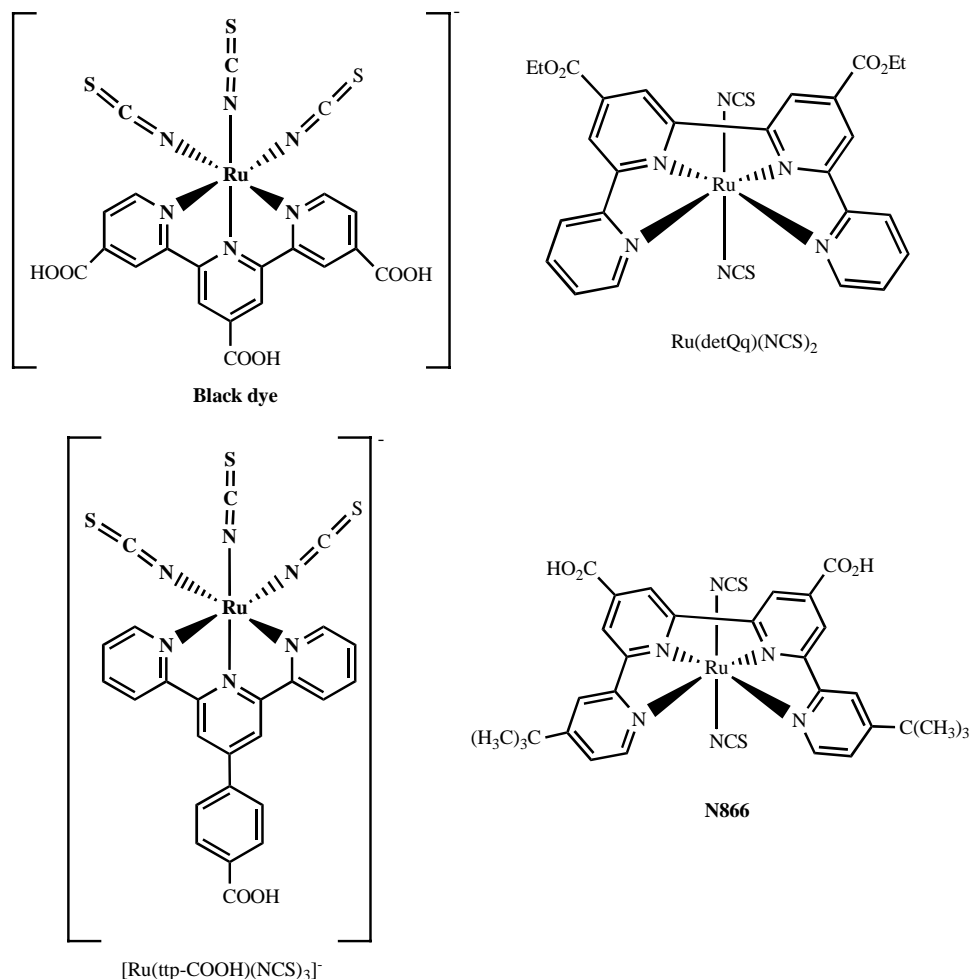[Ru(ttp-COOH)(NCS)$_3$]$^-$

N866

Fig. (14). Panchromatic sensitizers.

(**K8,** Fig. **15**) [72]. The lowest MLCT absorption maximum of **K8** is red-shifted 20 nm with molar extinction coefficient increased by 30% compared to the star sensitizer **N3** (Table **2**). The oxidation potential of **K8** is shifted cathodically by 0.05 V compared to the **N3** couple. This difference is due to the donor influence of 4,4'-bis-(carboxyvinyl)-2,2'-bipyridine relative to 4,4'-bis-(carboxy)-2,2'-bipyridine. The excited oxidation potential of complex **K8** is around -0.89V vs SCE, which is much more negative than TiO$_2$ conduction

Fig. (15). K8.

much more negative than TiO$_2$ conduction band [73]. The photocurrent action spectrum of the DSSC based on **K8** shows a broad response covering most of the visible spectrum. The IPCE values were 77% in the plateau region and strikingly, 66% even at 700 nm. The significant effect exerted by the ligand with extended conjugation is evident from the IPCE curve in the red region. The cell based on **K8** gave a photocurrent density of 18 mA/cm^2, an open circuit potential of 640 mV, a fill factor of 0.75, and an overall conversion efficiency of 8.64% under AM 1.5 sun light. The absorption data and the recombination dynamics for **K8** were observed to be indistinguishable from those for the **N3** dye, indicating that the insertion of the vinyl moiety in the anchoring ligand did not significantly reduce the electronic coupling between the dye and the TiO$_2$ electrode.

Islam *et al.* [74-76] designed a Ru quinolinyl complex, Ru(dcpq)$_2$(NCS)$_2$ (where dcpq is 2-(2-(4-carboxylic acid-pyridine)-4-carboxylic acid-quinoline), and some analogues with 4,4'-dicarboxylic acid-2,2'-biquinoline (dcbiq), 4,7-dicarboxylic acid-phenanthroline (dcphen) ligands. The lowest MLCT absorption maxima among them could be far red-shifted to 700 nm.

These typical dyes that can absorb light across the entire visible and NIR regions have been developed in recent molecular engineering. Initial results have indicated that these
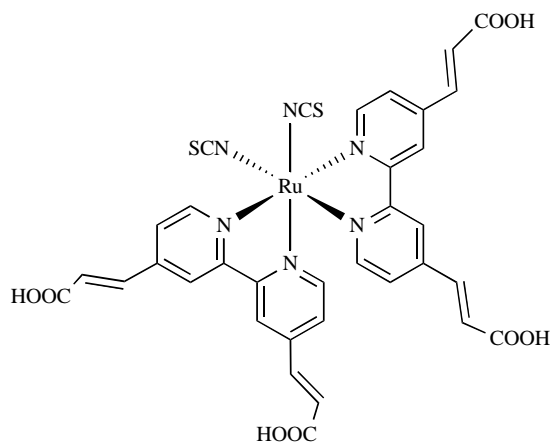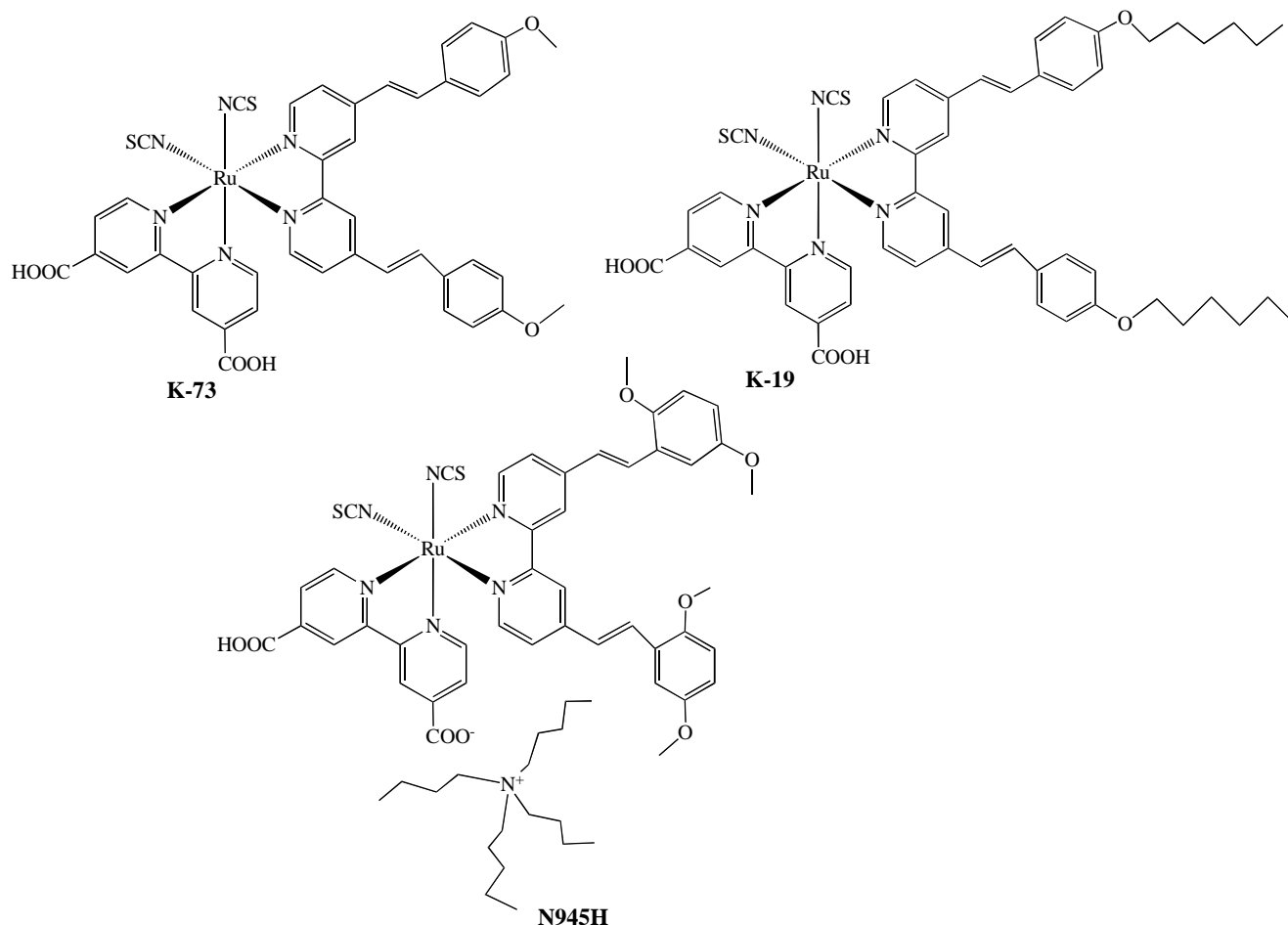
Fig. (16). Novel dyes with high molar extinction coefficient and good performance.

dyes may perform better photoelectric properties than **N3** once their performances have been optimized.

2.4. Increasing Molar Extinction Coefficients

For a DSSC, increasing the molar extinction coefficients of the sensitizers will enhance light harvesting with a given film thickness. Or thinner films can be designed to accomplish the same performance. Once the molar extinction coefficients are increased, it is possible to use the viscous electrolytes based on ionic liquids or nonvolatile solvents, resulting in better efficiencies with decreased losses during charge transport. The extinction coefficients of organic dyes [19, 77] are usually higher than transition-metal complexes. However, the disadvantages, such as narrow absorption bands [78], aggregation, and low stability, would limit the practical usage of such dyes in DSSC devices.

Very recently, a conversion efficiency of over 9% was obtained under AM 1.5 illumination for the DSSC based on the **K-73** sensitizer (Fig. **16**) with a nonvolatile electrolyte [79]. The **K-73** dye exhibited an intense absorption band in the visible region (the lowest MLCT band at λ=545 nm with ε=18000 cm^{-1}M^{-1}) because of the extension of π- conjugation on one of the bipiydyl ligands (Table **2**). Molecular orbital calculations indicate that the LUMO is located on the dcbH$_2$

ligand while the HOMO is shared by the Ru metal and NCS ligands.

The **K-19** (Fig. **16**) based DSSC in conjunction with the binary ionic liquid electrolyte gave a conversion efficiency of 7.1%. It exhibited better stability under both light soaking at 60 $^{\circ}$C and thermal stress at 80 $^{\circ}$C than the **K-73** dye [80, 81]. The adsorption of this dye on TiO$_2$ film was strengthened in the presence of the long alkyl chains. The nonvolatile electrolyte promoted the dye with high thermal stability in DSSCs. The molar extinction coefficient of ε=18200 cm^{-1}M^{-1} for the lowest MLCT absorption band at λ=543 nm for **K-19** is much higher than those for **Z907** and **N719** (ε=12200 cm^{-1}M^{-1} and 14000 cm^{-1}M^{-1} respectively)(Table **2**). The introduction of the alkoxystyryl moiety for **K-19** not only extended the conjugation of the bipyridine ligand, which greatly increased its molar extinction coefficient and solar light harvesting capacity, but also enhanced its hydrophobicity, which prevented water from desorbing the dye and stabilized the device performance under long-term light soaking and thermal stress.

As well, because of the extension of π- conjugation on the bipyidyl ligands, the molar extinction coefficient of **K8** (λ_{max} 555 nm, ε18000 M^{-1} cm^{-1}) was found to be much higher than that of **N3** (λ_{max} 535 nm, ε13600 M^{-1} cm^{-1}) [72].

Table 2. Typical Sensitizers, their Absorption Properties, Performances on DSSC

Sensitizer	Lowest MLCT Peak (nm)	Molar Extinction Coefficient($M^{-1}cm^{-1}$)	V_{oc}(mV)	I_{SC}(mA/cm^2)	FF	IPCE%	η%	Ref.
N3	535	14,000	720	18.2	0.73		10.00	[39]
Z907Na	526	12,200					6.00	[81]
K19	543	18,200	711	14.61	0.67		7.10	[99]
K73	545	18,000	748	17.22	0.69	85	9.00	[98]
N945	550	18,900	790	16.50	0.72	82	9.64	[101]
K8	550	18,000	640	18.00	0.75	77	9.64	[94]
trans-Ru	585		720	19.60			8.60	[88]
N886			680	11.80	0.73	40	5.85	[93]
Ru(H$_2$dcbpy)(dmbpy)(NCS)$_2$	524	11,600						[82]
Ru(H$_2$dcbpy)(dhbpy)(NCS)$_2$	525	11,100						[82]
Ru(H$_2$dcbpy)(dnbpy)(NCS)$_2$	526	11,600						[82]
Ru(H$_2$dcbpy)(dtdbpy)(NCS)$_2$	525	11,500	740	16.20	0.72	90	8.60	[82]
Ru(3,3'-dcbH$_2$)$_2$(NCS)$_2$	572		470	8.00		21		[64]
Ru(5,5'-dcbH$_2$)$_2$(NCS)$_2$	585		490	7.80		37		[64]
[Ru(ttp-COOH)(NCS)$_3$]$^-$	580		580	6.10		90	2.90	[40]
black dye	620		720	20.5		80	10.40	[38]
Ru(ttp-PO$_3$H$_2$)(dmbpy)(NCS)	503	8980	653	4.73	0.71	76		[75]
Ru(hp-terpy)(dmbpy)(NCS)	494	8700				70		[74]
Ru(bpy-(CH$_2$OH)$_2$)$_2$(NCS)$_2$			510	10	0.48		3.8	[82]
Ru(bpy-(PO$_3$H$_2$)$_2$)$_2$(NCS)$_2$	494	7000	490	5	0.67	~75		[78]
Ru(detOq)(NCS)$_2$	658	9800	654	18	0.65	~75		[90]

Another sensitizer, tetrabutylammonium ruthenium di-cyanato(4-carboxylic acid- 4'-carboxylate-2,2'-bipyridine)(4,4'-di(2-(3,6-dimethoxyphenyl)-ethenyl)-2,2'-bipyridine) (**N945H** in Fig. **16**), composed of different ligands with specific function was designed [82]. The 4,4'-di(2-(3,6-di-methoxyphenyl)-ethenyl)-2,2'-bipyridine ligand extended the π conjugation further. The function of such a ligand is to enhance the molar extinction coefficient and to tune the LUMO level of the sensitizer. The INDO/S and DFT calculations revealed that the charge was directed into the carboxylbipyridine ligand bound to the TiO$_2$ surface following photoexcitation. The hydrophobic group in the chromophore ligand of **N945** is very similar to that of **K-73**, in which only one methoxy group is attached on the para-position of the phenyl group. The lowest MLCT absorption band of **N945H** appears at 550 nm, with an extinction coefficient of 18900 M^{-1} cm^{-1}, which is significantly higher than the star sensitizer **N3** (Table **2**). The photovoltaic performance of the **N945** sensitized solar cell with a thermally stable electrolyte system (composed of 0.8 M 1,2-dimethyl-3-propylimidazolium iodide, 0.1 M I$_2$, and 0.5 M *N*-methylbenzimidazole in 3-methoxypropionitrile) was investigated. Strikingly, this DSSC generated a short-circuit photocurrent density of 16 mA cm^{-2}, an open-circuit potential of 752 mV, a fill factor of 0.69, and a power conversion efficiency of 8.4% under AM 1.5 full sunlight.

The pioneering work reveals that selective functioning of ruthenium complexes could result in red-shifted absorption spectra and enhanced molar extinction coefficients. This strategy provides the directionality to the molecular engineering of ruthenium sensitizers for DSSCs, especially for solid state DSSCs.

2.5. Increasing the Charge Separation and Minimizing the Charge Recombination

For the conversion of solar light into electrical current, an efficient charge separation must be achieved. The back electron transfer process from the conduction band of the titanium dioxide films to the oxidized sensitizer (eq. **6**) is undesirable. It generates heat instead of electrical current. For the characterization of the recombination rate, an important kinetic parameter is the rate constant k_6. It is of great importance to develop sensitizer systems with high value of k_1 and low value of k_6.

The charge separation in a DSSC is the key process during the generation of photocurrent. Either the **N3** or **N719** based DSSC is a good illustration. The forward electron injection is an extremely rapid process occurring in the femtosecond time domain. The back electron transfer involves a d orbital of the oxidized ruthenium complex localized on the ruthenium metal. The overlap of this d orbital and the conduction band of TiO_2 is small and is further reduced by the spatial contraction of the wave function upon oxidation of Ru(II) to Ru(III). Thus, the electronic coupling constant for the back electron transfer process is 1-2 orders of magnitude smaller than that for the forward electron injection process. The resulted spatial separation from the positive charge density on the dye from the injected electron has a crucial effect on retarding the charge recombination between the injected electron and the dye cation, which is a key loss process (Fig.1, k_6). Charge-recombination dynamics are closely dependent on this separation, and very little dependent on the thermodynamic driving force, as determined by the reduction potential of the dye cation [83].

The charge-recombination could be inhibited effectively by using **N845** (Fig. **17**), with attached electron-donor groups on the non-anchoring ligand, which can locate the cationic charge at a greater distant from the TiO_2 surface [84]. The **N845** sensitizer was designed by modification of the **N3**, in which a secondary electron donor moiety, *N,N*-(di-*p*-anisylamino)phenoxymethyl group was introduced. Following electron injection, the positive charge is transferred from the ruthenium ion to the triarylamine group, which moves the hole away from the surface. The increased distance retards the back electron transfer process. About a 1000-fold retardation of the recombination dynamics with an increased open circuit voltage (V_{oc}) for **N845** was attributed to the increase in distance between the cationic center and the TiO_2 surface (as estimated from semi-empirical calculations) in comparison with **N719**.
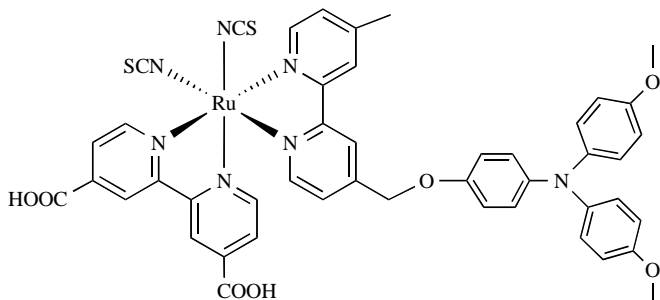
Fig. (17). N845.

Several research groups also tried to use dyes with electron-donor groups that could locate the cationic charge at a greater distant from TiO_2 surface [85, 86].

The photosensitization process of [Ru(dcbH$_2$)$_2$(4-CH$_3$, 4'-CH$_2$-PTZ-2,2'-bipyridine)]$^{2+}$ attached to TiO_2 was illustrated in Fig. **18**. Irradiation of the dye with visible light resulted in the creation of a MLCT excited state, and subsequently a charge separated state with an electron injected into TiO_2 and an oxidized PTZ group, abbreviated as $TiO_2(e^-)$–Ru–PTZ$^+$. Recombination of the electron in TiO_2

with the oxidized PTZ to generate the ground state occurred with a rate constant of 3.6×10^3 s^{-1}. Excitation of a model compound that does not contain the PTZ donor, [Ru(dmbpy)(dcbH$_2$)$_2$]$^{2+}$ (dmbpy = 4,4'-dimethyl-2,2'-bipyridine), under identical conditions gave rise to the immediate formation of a charge separated state, $TiO_2(e^-)$–Ru(III), whose recombination kinetics can be analyzed by a distribution model with an average rate of 3.9×10^6 s^{-1}. Therefore, transferring the "hole" from the Ru center to the pendant PTZ moiety inhibits the recombination rates about three orders of magnitude [87].
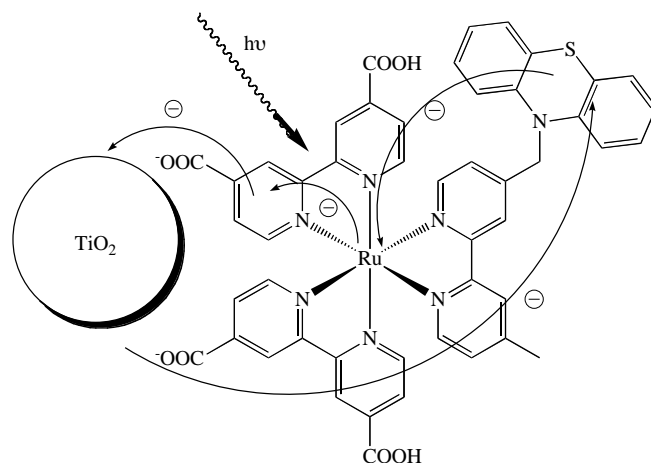

Fig. (18). Interfacial and intramolecular electron transfer processes in [Ru(dcbH$_2$)$_2$(4-CH$_3$,4'-CH$_2$-PTZ-2,2'-bipyridine)]$^{2+}$ anchored on TiO_2.

Ghanem *et al.* [88] designed a complex P$_{680}$ through mimicking the function of tyrosine and chlorophyll unit in natural photosystem II (PSII). A ruthenium(II) tris(bipyridyl) complex covalently linked to a L-tyrosine ethyl ester through an amide bond was attached to the surface of nanocrystalline TiO_2 *via* carboxylic acid groups on the bpy ligands. Excitation of the complex promotes a metal-to-ligand charge-transfer (MLCT) excited state, from which an electron was injected into the conduction band of TiO_2. An intramolecular electron transfer occurred subsequently from tyrosine to Ru(III), regenerating Ru(II) and forming the tyrosyl radical.

Some heterosupramolecular systems like binuclear ruthenium and osmium containing polypyridyl complexes [89, 90], TiO_2-Re-Ru [91], TiO_2-Rh-Ru [92] were employed to study the interfacial and intramolecular electron transfer process.

2.6. Strategies for the Stability of the Sensitizers on the Mesoscopic Films

Although it's necessary for the sensitizers with carboxylic acid groups to anchor on the surface of the TiO_2, this adsorption is susceptible to the trace amount of water, causing serious consequences on the long-term stability of the DSSCs. It has been reported that the dyes with hydrophobic chains (e.g. **Z907, Z955**) can display an enhanced stability towards desorption from TiO_2 induced by water in the liquid or gel electrolyte [93, 94]. A cell based on **Z907** with an I$^-$/I$_3^-$ couple in polymer gel gave a conversion efficiency of 6.1%, with excellent stability to both prolonged thermal stress and
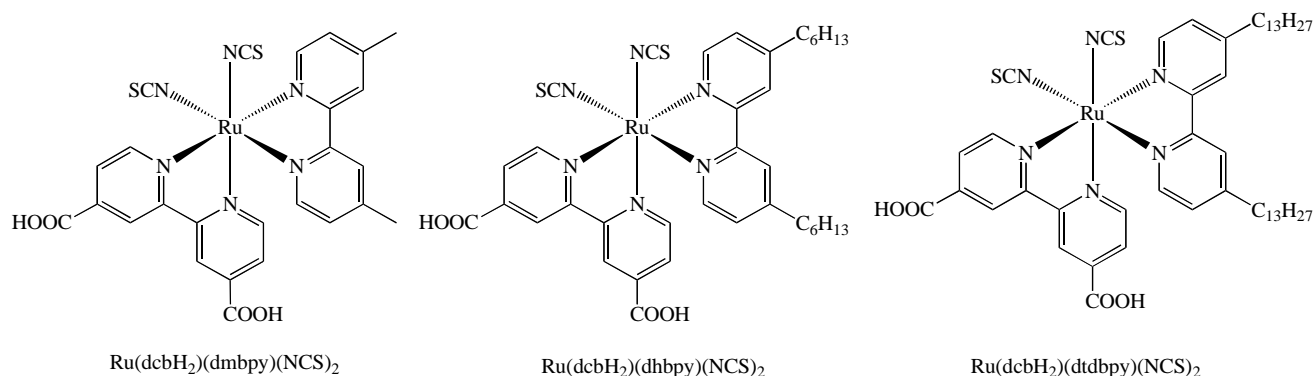
Ru(dcbH₂)(dmbpy)(NCS)₂   Ru(dcbH₂)(dhbpy)(NCS)₂   Ru(dcbH₂)(dtdbpy)(NCS)₂

Fig. (18). The amphiphilic heteroleptic Ru(II) complexes.

light soaking that satisfied the criteria for the outdoor use of solar cells (Table **2**) [95]. The stability was attributed to the hydrophobic property of the dye and the stability of the gel electrolyte. The DSSC based on **N719** displayed much poorer stability and thermal stress compared to **Z907**. The **K-19** and **K-73** dyes are similar examples that exhibited much better light-soaking stabilities and thermal stress than the **N3** dye.

A series of amphiphilic heteroleptic Ru(II) complexes with different length of chains on the 2,2'-bipyridine ligand, such as Ru(dcbH₂)(dmbpy)(NCS)₂, Ru(dcbH₂)(dhbpy) (NCS)₂, Ru(dcbH₂)(dtdbpy)(NCS)₂ (Fig. **19**) and **Z907** (Fig. **9**), were developed. Their spectroscopic properties and the photovoltaic performances as well as stabilities of the corresponding DSSCs were compared with those of **N3** [96]. Their lowest MLCT absorption bands were blue shifted with molar extinction coefficients decreased when compared to those of the **N3** (Table **2**). The ruthenium oxidation potentials in complex **Z907** and Ru(dcbH₂)(dtdbpy)(NCS)₂ are shifted negatively by 0.11V, compared to that in **N3**. The difference in the oxidation potential is due to the presence of 4,4'-nonyl-2,2'-bpy in **Z907**, which is a stronger donor compared to the 4,4'-dicarboxylic acid-2,2'-bipyridine. Under identical conditions, the short circuit photocurrent density, the open circuit voltage, and the cell efficiency increased slightly with the increase in chain length of the ligand among these amphiphilic dyes based DSSCs. Most importantly, the power conversion efficiency of the cell was sustained at 94% of its initial value upon heating for 1000 h at 80°C for the **Z907**. These results reveal that it is promising to develop stable sensitizers for the application in DSSCs *via* molecular engineering. Another advantage for dyes with hydrophobic groups is that the hydrophobic groups can inhibit the recombination of electrons on the TiO₂ conduction band with the redox electrolyte (see eq. **5**, known as dark current) by forming a hydrophobic network. Evidence indicates that **N719** itself can suppress the dark current by forming a blocking layer on the TiO₂ surface [50, 95]. This effect may be enhanced further *via* introducing of bulk substitutes to the dye.

Such amphiphilic dyes can be applied in DSSCs with an organic hole transport material instead of the liquid electrolyte I⁻/I₃⁻. In such cells, the poor interaction between the sensitizer and the organic hole transport materials [98] would result in a weaker electronic communication and a slow re-

generation of the ground state sensitizer. Sensitizers with hydrophobic chains can enhance the stability of DSSCs *via* enhancing the interaction between TiO₂ and the sensitizer. Interfacial electron transfer process between the sensitizer and the hole transport material is also important in the development of solid DSSCs [99], especially for the high-molecular-weight polymers that do not penetrate well into the nanopores of the TiO₂ semiconductor. It is also interesting to note that a typically slow k_2 in the DSSCs with an organic hole transport material requires the sensitizer having a long-term stability in their oxidized form [67].

3. SUMMARY

The DSSCs are considered as the new generation solar cells for the 21st century. Much work has been done towards the optimization of the performance of the cells for the commercial application in the near future. Although the well established Ru complexes **N3**, **N719**, "**black dye**" exhibit high efficiencies in the standard dye-sensitized solar cell with an I⁻/I₃⁻ solution electrolyte, there are still some limits for the massive production. It is promising to design the high efficient, panchromatic, and stable sensitizers for the DSSC *via* the molecular engineering of the sensitizers.

ACKNOWLEDGEMENT

REFERENCES

[1]   Grätzel, M. *Nature,* **2001**, *414*, 338.
[2]   Nakade, S.; Saito, Y.; Kubo, W.; Kitamura, T.; Wada, Y.; Yanagida, S. *J. Phys. Chem. B,* **2003**, *107*, 8607.
[3]   Palomares, E.; Clifford, J. N.; Haque, S. A.; Lutz, T.; Durrant, J. R. *J. Am. Chem. Soc.,* **2003**, *125*, 475.
[4]   Hara, K.; Sato, T.; Katoh, R.; Furube, A.; Ohga, Y.; Shinpo, A.; Suga, S.; Sayama, K.; Sugihara, H.; Arakawa, H. *J. Phys. Chem. B,* **2003**, *107*, 597.
[5]   Benkstein, K. D.; Kopidakis, N.; van de Lagemaat, J.; Frank, A. J. *J. Phys. Chem. B,* **2003**, *107*, 7759.
[6]   Qiu, F. L.; Fisher, A. C.; Walker, A. B.; Petecr, L. M. *Electrochem. Commun.,* **2003**, *5*, 711.
[7]   He, J.; Benko, G.; Korodi, F.; Polivka, T.; Lomoth, R.; Akermark, B.; Sun, L.; Hagfeldt, A.; Sundstrom, V. *J. Am. Chem. Soc.,* **2002**, *124*, 4922.
[8]   Nazeeruddin, M. K.; Gratzel, M. In *Comprehensive Coordination Chemistry II,* (Eds.: McCleverty J. A.; Meyer T. J.), Elsevier, Dordrecht, **2004**, Vol. *9,* chap. 16.
[9]   Hagsfeldt, A.; Grätzel, M. *Chem. Rev.,* **1995**, *95*, 49.

[10]   Bedja, I.; Hotchandani, S.; Carpentier, R.; Fessenden, R.W.; Kamat, P.V. *J. Appl. Phys*., **1994**, *75*, 5444.

[11]   Boschloo, G. K.; Goossens, A. *J. Phys. Chem.,* **1996**, *100*, 19489.

[12]   Nazeeruddin, Md. K.; Humphry-Baker, R.; Grätzel, M.; Murrer, B.A. *J. Chem. Soc. Chem. Commun.,* **1998**, 719.

[13]   Cinnsealach, R.; Boschloo, G.; Rao, S.N.; Fitzmaurice, D. *Solar Energy Mater. Solar Cells,* **1999**, *57*, 107.

[14]   Meyer, T. J.; Meyer, G. J.; Pfennig, B. P.; Schoonover, J. R.; Timpson, C. J.; Wall, J. F.; Kobusch, C.; Chen, X.; Peek, B.M.; Wall, C. J.; Ou, W.; Erickson, B.W.; Bignozzi, C.A. *Inorg. Chem*., **1994**, *33*, 3952.

[15]   Fujihira, M. *Mol. Cryst. Liq. Cryst.,* **1990**, *183*, 59.

[16]   Ramakrishna, G.; Gosh, H.N. *J. Phys. Chem. B,* **2001**, *105*, 7000.

[17]   Martini, I.; Hodak, J.H.; Hartland, G.V. *J. Phys. Chem. B*, **1998**, *102*, 9508.

[18]   Huber, R.; Spörlein, S.; Moser, J.E.; Grätzel, M.; Wachtveitl, J. *J. Phys. Chem. B*, **2000**, *104*, 8995.

[19]   Hara, K.; Wang, Z.-S.; Sato, T.; Furube, A.; Katoh, R.; Sugihara, H.; Dan-oh, Y.; Kasada, C.; Shinpo, A.; Suga, S. *J. Phys. Chem. B,* **2005**, *109*, 15476.

[20]   Alex, S.; Santhosh, U.; Das, S. *J. Photochem. Photobiol. A,* **2005**, *172*, 63.

[21]   Horiuchi, T.; Miura, H.; Sumioka, K.; Uchida, S. *J. Am. Chem. Soc.,* **2004**, *126*, 12218.

[22]   Chen, Y.-S.; Li, C.; Zeng, Z.-H.; Wang, W.-B.; Wang, X.-S.; Zhang, B.-W. *J. Mater. Chem.*, **2005**, *15*, 1654.

[23]   Dai, Q.; Rabani, J. *New J. Chem.,* **2002**, *26,* 421.

[24]   Olea, A.; Ponce, G.; Sebastian, P.J. *Sol. Energy Mater. Sol. Cells,* **1999**, *59,* 137.

[25]   Cherepy, N.J.; Smestad, G.P.; Grätzel, M.; Zhang, J.Z. *J. Phys. Chem. B.,* **1997**, *101*, 9342.

[26]   Tennakone, K.; Kumarasinghe, A.R.; Kumara, G.R.R.A.; Wijayantha, K.G.U.; Sirimanne, P.M. *J. Photochem. Photobiol. A,* **1997**, *108*, 193.

[27]   Garcia, C.G.; Polo, A.S.; Murakami Iha, N.Y. *J. Photochem. Photobiol. A*, **2003**, 160, 87.

[28]   Balzani, V.; Juris, A.; Venturi, M.; Campagna, S.; Serroni, S. *Chem. Rev*., **1996**, *96*, 759.

[29]   Regan, B. O.; Grätzel, M. *Nature*, **1991**, *353*, 737.

[30]   Nazeeruddin, M. K.; Pechy, P.; Renouard, T.; Zakeeruddin, S. M.; Humphrey-Baker, R.; Comte, P.; Liska, P.; Cevey, L.; Costa, E.; Shklover, V.; Spiccia, L.; Deacon, G. B.; Bignozzi, C. A.; Grätzel, M. *J. Am. Chem. Soc*., **2001**, *123*, 1613.

[31]   Nazeeruddin, M. K.; Kay, A.; Rodicio, I.; Humphry-Baker, R.; Muller, E.; Liska, P.; Vlachopoulos, N.; Grätzel, M. *J. Am. Chem. Soc.,* **1993**, *115*, 6382.

[32]   Hara, K.; Sugihara, H.; Singh, L.P.; Islam, A.; Katoh, R.; Yanagida, M.; Sayama, K.; Murata, S.; Arakawa, H. *J. Photochem. Photobiol. A,* **2001**, *145*, 117.

[33]   Hara, K.; Sugihara, H.; Tachibana, Y.; Islam, A.; Yanagida, M.; Sayama, K.; Arakawa, H.; Fujihashi, G.; Horiguchi, T.; Kinoshita, T. *Langmuir*, **2001**, *17*, 5992.

[34]   Wang, Z.-S.; Huang, C.-H.; Huang, Y.-Y.; Zhang, B.-W.; Xie, P.-H.; Hou, Y.-J.; Ibrahim, K.; Qian, H.-J.; Liu, F.-Q. *Sol. Energy Mater. Sol. Cells,* **2002**, *71*, 261.

[35]   Yao, Q.-H.; Huang, Y.-Y.; Song, L.-Q.; Zhang, B.-W.; Huang, C.-H.; Wang, Z.-S.; Li, F.-Y.; Zhao, X.-S. *Sol. Energy Mater. Sol. Cells,* **2003**, *77*, 319.

[36]   Grätzel, M. *Inorg. Chem*., **2005**, *44*, 6841.

[37]   Sugihara, H.; Singh, L.P.; Sayama, K.; Arakawa, H.; Nazeeruddin, M.K.; Grätzel, M. *Chem. Lett.,* **1998**, 1005.

[38]   Yanagida, M.; Singh, L.P.; Sayama, K.; Hara, K.; Katoh, R.; Islam, A.; Sugihara, H.; Arakawa, H.; Nazeeruddin, M.K.; Grätzel, M. *J. Chem. Soc. Dalton Trans*., **2000**, 2817.

[39]   Schwarz, O.; van Loyen, D.; Jockusch, S.; Turro, N.J.; Dürr, H. *J. Photochem. Photobiol. A,* **2000**, *132*, 91.

[40]   Islam, A.; Sugihara, H.; Hara, K.; Singh, L.P.; Katoh, R.; Yanagida, M.; Takahashi, Y.; Murata, S.; Arakawa, H. *J. Photochem. Photobiol. A,* **2001**, *145*, 135.

[41]   Nazeeruddin, M.K.; Müller, E.; Humphry-Baker, R.; Vlachopoulos, N.; Grätzel, M. *J. Chem. Soc. Dalton Trans*., **1997**, 4571.

[42]   Yanagida, M.; Islam, A.; Tachibana, Y.; Fujihashi, G.; Katoh, R.; Sugihara, H.; Arakawa, H. *New J. Chem*., **2002**, *6*, 963.

[43]   Kalyanasundaram, K.; Grätzel, M. *Coord. Chem. Rev.,* **1998**, *177*, 347.

[44]   Vittadini, A.; Selloni, A.; Rotzinger, F.P.; Grätzel, M. *J. Phys. Chem. B,* **2000**, *104*, 1300.

[45]   Wang, P.; Klein, C.; Moser, J. E.; Humphrey-Baker, R.; Cevey-Ha N.-L.; Charvet, R.; Comte, P.; Zakeeruddin, S. M.; Grätzel, M. *J. Phys. Chem. B,* **2004**, *108*, 17553.

[46]   Hou, Y.; Xie, P.; Zhang, B.; Cao, Y.; Xiao, X.; Wang, W. *Inorg. Chem.,* **1999**, *38,* 6320.

[47]   Galoppini, E. *Coord. Chem. Rev.,* **2004**, *248,* 1283.

[48]   Altobello, S.; Bignozzi, C. A.; Caramori, S.; Larramona, G.; Quici, S.; Marzanni, G.; Lakhmiri, L. R. *J. Photochem. Photobiol. A,* **2004**, *166*, 91.

[49]   Xie, P.-H.; Hou, Y.-J.; Wei, T.-X.; Zhang, B.-W.; Cao, Y.; Huang, C.-H. *Inorg. Chim. Acta,* **2000**, *308,* 73.

[50]   Geary, E. A. M.; Yellowlees, L. J.; Jack, L. A.; Oswald, I. D. H.; Parsons, S.; Hirata, N.; Durrant, J. R.; Robertson, N. *Inorg. Chem*., **2005**, *44*, 242.

[51]   Pechy, P.; Rotzinger, F.P.; Nazeeruddin, M.K.; Kohle, O.; Zakeeruddin, S.M.; Humphry-Baker, R.; Grätzel, M. *Chem. Commun.*, **1995**, 65.

[52]   Zakeeruddin, S.M.; Nazeeruddin, M.K.; Pechy, P.; Rotzinger, F.P.; Humphry-Baker, R.; Kalyanasundaram, K.; Grätzel, M.; Shklover, V.; Haibach, T. *Inorg. Chem.,* **1997**, *36*, 5937.

[53]   Jing, B.W.; Zhang, H.; Zhang, M.H.; Lu, Z.H.; Shen, T. *J. Mater. Chem*., **1998**, *8*, 2055.

[54]   Gillaizeau-Gauthier, I.; Odobel, F.; Alebbi, M.; Argazzi, R.; Costa, E.; Bignozzi, C.A.; Qu, P.; Meyer, G. J. *Inorg. Chem.,* **2001**, *40*, 6073.

[55]   Argazzi, R.; Bignozzi, C. A.; Heimer, T. A.; Castellano, F. N.; Meyer, G. J. *Inorg. Chem*., **1994**, *33*, 5741.

[56]   Zabri, H.; Gillaizeau-Gauthier, I.; Bignozzi, C.A.; Caramori, S.; Charlot, M.-F.; Boquera, J.-C.; Odobel, F. *Inorg. Chem*., **2003**, *42*, 6655.

[57]   Nazeeruddin, M. K.; Zakeeruddin, S. M.; Humphrey-Baker, R.; Jirousek, M.; Liska, P.; Vlachopoulos, N.; Shklover, V.; Fischer, C.-H.; Grätzel, M. *Inorg. Chem.,* **1999**, *38*, 6298.

[58]   Yanagida, M.; Yamaguchi, T.; Kurashige, M.; Hara, K.; Katoh, R.; Sugihara, H.; Arakawa, H. *Inorg. Chem.,* **2003**, *42*, 7921.

[59]   Sauve, G.; Cass, M. E.; Doig, S. J.; Lauermann, I.; Pomykal, K.; Lewis, N. S. *J. Phys. Chem. B,* **2000**, *104*, 3488.

[60]   Heimer, T. A.; Heilweil, E. J.; Bignozzi, C. A.; Meyer, G. J. *J. Phys. Chem. A,* **2000**, *104*, 4256.

[61]   Islam, A.; Sugihara, H.; Hara, K.; Singh, L.P.; Katoh, R.; Yanagida, M.; Takahashi, Y.; Murata, S.; Arakawa, H. *J. Photochem. Photobiol. A,* **2001**, *145*, 135.

[62]   Anandan, S.; Latha, S.; Maruthamuthu, P. *J. Photochem. Photobiol. A,* **2002**, *150*, 167.

[63]   Takahashi, Y.; Arakawa, H.; Sugihara, H.; Hara, K.; Islam, A.; Katoh, R.; Tachibana, Y.; Yanagida, M. *Inorg. Chim. Acta,* **2000**, *310*, 169.

[64]   Lees, A. C.; Evrard, B.; Keyes, T. E.; Vos, J.G.; Kleverlaan, C. J.; Alebbi, M.; Bignozzi, C. A. *Eur. J. Inorg. Chem*., **1999**, 2309.

[65]   Wang, Z.; Huang, C.; Zhang, B.; Hou, Y.; Xie, P.; Qian, H.; Ibrahim, K. *New J. Chem.,* **2000**, *24, 567.*

[66]   Zakeeruddin, S.M.; Nazeeruddin, Md. K.; Humphry-Baker, R.; Grätzel, M. *Inorg. Chim. Acta,* **1999**, *296*, 250.

[67]   Argazzi, R.; Larramona, G.; Contado, C.; Bignozzi, C. A. *J. Photochem. Photobiol. A,* **2004**, *164*, 15.

[68]   Kuciauskas, D.; Freund, M.S.; Gray, H.B.; Winkler, J.R.; Lewis, N.S. *J. Phys. Chem. B,* **2001**, *105,* 392.

[69]   Sauvè, G.; Cass, M.E.; Coia, G.; Doig, S.J.; Lauermann, I.; Pomykal, K.E.; Lewis, N.S. *J. Phys. Chem. B,* **2000**, *104*, 6821.

[70]   Renouard, T.; Fallahpour, R.-A.; Nazeeruddin, M. K.; Humphrey-Baker, R.; Gorelsky, S. I.; Lever, A. B. P.; Grätzel, M. *Inorg. Chem.,* **2002**, *41*, 367.

[71]   Barolo, C.; Nazeeruddin, Md. K.; Fantacci, S.; Di Censo, D.; Comte, P.; Liska, P.; Viscardi, G.; Quagliotto, P.; De Angelis, F.; Ito, S.; Grätzel, M. *Inorg. Chem.,* **2006**, *45,* 4642.

[72]   Klein, C.; Nazeeruddin, Md. K.; Liska, P.; Di Censo, D.; Hirata, N.; Palomares, E.; Durrant, J. R.; Grätzel, M. *Inorg. Chem.*, **2005**, *44*, 178.

[73]   Liu, G.; Jaegermann, W.; He, J.; Sundstrom, V.; Sun, L. *J. Phys. Chem. B,* **2002**, *106*, 5814.

[74]   Islam, A.; Sugihara, H.; Singh, L. P.; Hara, K; Katoh, R.; Nagawa, Y.; Yanagida, M.; Takahashi, Y.; Murata, S.; Arakawa, H. *Inorg. Chim. Acta*, **2001**, *322*, 7.

[75]   Islam, A.; Hara, K.; Singh, L. P.; Katoh, R.; Yanagida, M.; Murata, S.; Takahashi, Y.; Sugihara, H.; Arakawa, H. *Chem. Lett.*, **2000**, *5*, 490.

[76]   Islam, A.; Sugihara, H.; Yanagida, M.; Hara, K.; Fujihashi, G.; Tachibana, Y.; Katoh, R.; Murata Arakawa, H. *New J. Chem.* **2002**, *26*, 966.

[77]   Thomas, K. R. J.; Lin, J. T.; Hsu, Y.-C.; Ho, K.-C. *Chem. Commun.*, **2005**, 4098.

[78]   Chen, Y.; Zeng, Z.; Li, C.; Wang, W; Wang, X.; Zhang, B. *New J. Chem.*, **2005**, *29*, 773.

[79]   Kuang, D.; Ito, S.; Wenger, B.; Klein, C.; Moser, J. E.; Humphry-Baker, R.; Zakeeruddin, S. M.and Grätzel M. *J. Am. Chem. Soc.*, **2006**, *128*, 4147.

[80]   Wang, P.; Klein, C.; Humphry-Baker, R.; Zakeeruddin, S. M.; Grätzel, M. *J. Am. Chem. Soc.*, **2005**, *127*, 808.

[81]   Wang, P.; Klein, C.; Humphry-Baker, R.; Zakeeruddin, S. M.; Grätzel, M. *Appl. Phys. Lett.*, **2005**, *86*, 123508.

[82]   Nazeeruddin, M. K.; Wang, Q.; Cevey, L.; Aranyos, V.; Liska, P.; Figgemeier, E.; Klein, C.; Hirata, N.; Koops, S.; Haque, S. A.; Durrant, J. R.; Hagfeldt, A.; Lever, A. B. P.; Grätzel, M. *Inorg. Chem.*, **2006**, *45*, 787.

[83]   Clifford, J. N.; Palomares, E.; Nazeeruddin, M. K.; Grätzel, M.; Nelson, J.; Li, X.; Long, N. J.; Durrant, J. R. *J. Am. Chem. Soc.*, **2004**, *126*, 5225.

[84]   Hirata, N.; Lagref, J.-J.; Palomares, E. J.; Durrant, J. R.; Nazeeruddin, M. K.; Grätzel, M.; Di Censo, D. *Chem. Eur. J.*, **2004**, *10*, 595.

[85]   Argazzi, R.; Bignozzi, C. A. *J. Am. Chem. Soc.*, **1995**, *117*, 11815.

[86]   Clifford, J. N.; Yahioglu, G.; Milgrom, L. R.; Durrant, J. R. *Chem. Commun.*, **2002**, 1260.

[87]   Argazzi, R.; Bignozzi, C.A.; Heimer, T.A.; Castellano, F.N.; Meyer, G. J. *J. Phys. Chem. B*, **1997**, *101*, 2591.

[88]   Ghanem, R.; Xu, Y.; Pan, J.; Hoffmann, T.; Andersson, J.; Polívka, T.; Pascher, T.; Styring, S.; Sun, L. Sundström L. *Inorg. Chem.*, **2002**, *41*, 6258.

[89]   Kleverlaan, C. J.; Alebbi, M.; Argazzi, R.; Bignozzi, C. A.; Hasselmann, G.M.; Meyer, G. J. *Inorg. Chem.*, **2000**, *39*, 1342.

[90]   Lees, A.C.; Kleverlaan, C. J.; Bignozzi, C.A.; Vos, J.G. *Inorg. Chem.*, **2001**, *40*, 5343.

[91]   Argazzi, R.; Bignozzi, C.A.; Heimer, T.A.; Meyer, G. J., *Inorg. Chem.*, **1997**, *36*, 2.

[92]   Kleverlaan, C.J.; Indelli, M.T.; Bignozzi, C.A.; Pavanin, L.; Scandola, F.; Hasselmann, G.M.; Meyer, G. J. *J. Am. Chem. Soc.*, **2000**, *122*, 2840.

[93]   Wang, P.; Zakeeruddin, S. M.; Moser, J. E.; Nazeeruddin, M. K.; Sekiguchi, T.; Grätzel, M. *Nat. Mater.*, **2003**, *2*, 402.

[94]   Zakeeruddin, S. M.; Nazeeruddin, M. K.; Humphry-Baker, R.; Pechy, P.; Quagliotto, P.; Barolo, C.; Viscardi, G.; Grätzel, M. *Langmuir*, **2002**, *18*, 952.

[95]   Ito, S.; Liska, P.; Comte, P.; Charvet, R.; Pechy, P.; Bach, U.; Schmidt-Mende, L.; Zakeeruddin, S. M.; Kay, A.; Nazeeruddin, M. K. , Grätzel, M. *Chem. Commun.*, **2005**, 4351.

[96]   Nazeeruddin, Md. K.; Zakeeruddin, S.M.; Lagref, J.-J.; Liska, P.; Comte, P.; Barolo, C.; Viscardi, G.; Schenk, K.; Grätzel, M. *Coord. Chem. Rev.*, **2004**, *248*, 1317.

[97]   Klein, C.; Nazeeruddin, Md. K.; Di Censo, D.; Liska, P.; Grätzel, M. *Inorg. Chem.*, **2004**, *43*, 4216.

[98]   Saito, Y.; Fukuri, N.; Senadeera, R.; Kitamura, T.; Wada, Y.; Yanagida, S. *Electrochem. Commun.*, **2004**, *6*, 71.

[99]   Kang, M.-S.; Kim, J. H.; Kim, Y. J.; Won, J.; Park, N.-G.; Kang, Y. S. *Chem. Commun.*, **2005**, 889.